

Sol-Gel Production of ZrO₂ and 8YSZ with New Organic Precursor

Crina Suciu^{a,*} Alex C. Hoffmann^a Lucia Gagea^b

^a*Department of Physics and Technology, The University of Bergen
Allégaten 55, 5007 Bergen, Norway*

^b*Faculty of Chemistry and Chemical Engineering, 400028, Cluj-Napoca, Romania*

Abstract

In the present work ZrO₂ and 8YSZ nanoparticles were obtained by the sol-gel method using both conventional and new organic precursors. The new precursors (sucrose and pectin) have the advantage of being ubiquitous, cost-effective and non-toxic. The obtained particles are compared, and those obtained with the new precursors are shown to be smaller than those obtained using conventional precursors (citric acid, ethylene glycol and glycerol). X-ray diffraction (XRD) was used to determine the chemical composition and the crystal structure, and thermal analysis (TA) to determine the chemical and physical properties of the samples. The mean particle/crystallite size was determined by Transmission Electron Microscopy (TEM) and from the XRD data using the Scherrer formula. Single and multi-point BET analysis were performed in order to determine the specific surface area. Results of these analyses are presented in the paper.

Key words: Nanoparticles, Zirconia particles, Yttrium stabilized zirconia, Sol-gel, Particle size, Crystal structure

PACS: 81.07.-b, 81.05.-t, 81.20.-n, 81.07.Wx

* Corresponding author.

Email address: crina.suciu@ift.uib.no (Crina Suciu).

1 Introduction

Nanoscale oxide powders with particles of uniform shapes and narrow size distribution have gained increasing interest, among other things for the development of functional ceramics. In the past few years many production processes for nanoparticles have been introduced. We are interested in chemical production methods here, chemical methods include precipitation, co-precipitation and sol-gel methods [1–8]. Many functional ceramics are based on zirconium oxide ZrO_2 . Zirconium oxide has the three stable crystal forms shown in Figure 1.



Fig. 1. Stable phases of ZrO_2

The tetragonal phase may exist as a metastable phase down to ambient temperatures. The transitions between these phases and the attendant volume changes can be problematic. To avoid this ZrO_2 may be doped with some other oxide (e.g. MgO , CaO , Y_2O_3) to slow or eliminate the phase changes. In this paper we study—in addition to pure ZrO_2 —also ZrO_2 doped with Y_2O_3 . This doping stabilizes the cubic crystal structure right down the ambient temperatures, and moreover gives rise to oxygen vacancies making the material ionically conductive and suitable for use in fuel cells and oxygen sensors. A few articles study the production of ZrO_2 nanoparticles with the sol-gel process. The crystallization of ZrO_2 in ZrO_2 - SiO_2 mixtures have been studied using X-ray crystallography (XRD), differential thermal analysis (DTA) and electron microscopy [9–11]. Tetragonal and monoclinic ZrO_2 phases were identified. Ong et al. [12] studied specifically the crystallization behavior of sol-derived nanoparticles of pure ZrO_2 with DTA and XRD. Oleshko et al. [13] used a number of analytical techniques to study the metastable tetragonal phase in nanocrystalline pure ZrO_2 powders. They found tetragonal metastable phase in particles up to 100 nm, considerably larger than previously reported. We finally mention the study of Mehta et al. [14], who studied the formation of sol-gel derived yttria-stabilized zirconia films of for fuel cells using TGA.

2 Experimental Work

$\text{Zr}(\text{NO}_3)_2 \cdot x\text{H}_2\text{O}$ (Aldrich-Sigma, purity = 99.99%) was used as ZrO_2 precursor in all the samples. Citric acid monohydrate (Merck, Germany), ethylene glycol (Mallinckrod Baker B.V.), glycerol (anhydrous pure, Merck, Germany), commercial sucrose and pectin were used as organic precursors. A water based solution (Solution I) of $\text{Zr}(\text{NO}_3)_2 \cdot x\text{H}_2\text{O}$ (conc. 5g/l) was prepared in order to obtain the ZrO_2 powders. In the case of 8YSZ powders, $\text{Y}(\text{NO}_3)_3 \cdot 6\text{H}_2\text{O}$ (Sigma-Aldrich, 99.9% purity) was used for ZrO_2 stabilization. The appropriate quantity for a final composition of 8mol% Y_2O_3 to ZrO_2 was calculated and used. To complete Solution I, Nitric

Acid was added (conc = 65%, Riedel-de Haen) in a salt solution:acid volumetric ratio of 20:1. The pH of the final Solution I was 0.5–1. Another aqueous solution (Solution II) was prepared by dissolving the organic precursors in the amounts shown in Table 1 as multiples of the zirconium salt quantity. The final solutions I and II were homogenized together on a warming plate (100–120°C) and from the transparent homogenized solution the sol and the gel were gradually formed. The heating treatment was continued until a dried gel was obtained. The calcination temperature was 900°C for all the samples, at a heating rate of 100°C/min with one-hour plateaus at 500 and 900°C.

Table 1

The organic precursor:zirconium salt mass ratios used

Sample	Citric Acid (CA)	Ethylene Glycol (EG)	Glycerol (G)	Sucrose:pectin (SP)
Mass ratio	100:1	78:1	100:1	12:1:1

3 Results and Discussion

3.1 Thermal Analysis

Small dried gels of the two samples using sucrose/pectin organic precursors (ZrO₂ and 8YSZ) were studied by Thermal Analysis using a Derivatograph Q 1500 (MOM Hungary). The dried gels were analyzed at a heating rate of 10°C/min and the results are shown in Figure 2. Analysing the TG and TDG curves of the ZrO₂ samples shows that a 5% mass reduction occurs between 100 and 200°C (due to water elimination). Between 200 and 550°C an exothermic process takes place with 60% mass reduction due to the decomposition of the organic components. On the DTA curve the exothermic process can be seen to continue with relatively constant intensity up to 950°C attributed to the formation of ZrO₂. At 950°C all the processes are finished and the total losses are about 80% of the initial mass. For the YSZ dried

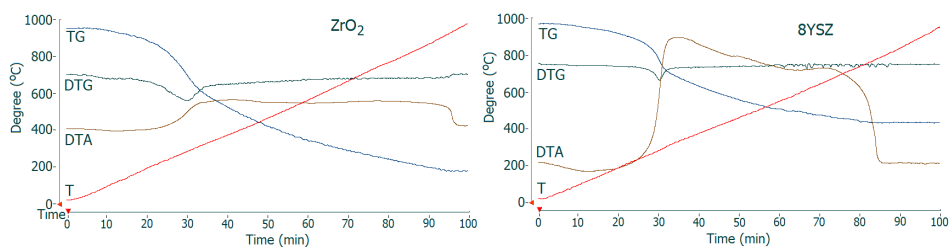


Fig. 2. The thermal analysis of the sucrose/pectin samples

gel the TG curve shows a process with a mass loss of 3–4% at 100°C which takes place with low speed due to water elimination. A strong exothermic process takes

place between 280-300°C (due to the organic compound oxidation) and continues up to 850°C with a slight inflection at 650°C attributed to the formation of ZrO₂ and of the solid solution between ZrO₂ and Y₂O₃ required to obtain the cubic form. At 900°C all the processes are finished and the total mass losses are about 55%.

3.2 Specific Surface Area

The specific surface area was determined from nitrogen adsorption using a Gemini 2380 from Micromeritics. All the samples were degassed at 300°C for 3 hours under vacuum before analysis. The obtained BET values of the specific surface area for all the samples are shown in Table 2. The standard deviations were calculated on basis of the multipoint analyses by the data acquisition software of the instrument (using Gauss' error propagation formula). The particle sizes were calculated using

Table 2
The specific surface areas of the samples at 900°C

Sample	BET Singlepoint	BET Multipoint	Standard Deviation
	[m ² /g]	[m ² /g]	
Citric acid (CA)	11.12	12.14	±0.053
Ethylene glycol (EG)	7.28	7.87	±0.033
Glycerol (G)	8.32	8.77	±0.037
Sucrose (S)	17.00	18.31	±0.056
YSZ sucrose	20.40	21.28	±0.084

the density of the cubic ZrO₂ of 6270 kg/m³, tetragonal ZrO₂ of 6100 kg/m³ and monoclinic + tetragonal ZrO₂ of 5600 kg/m³ and assuming that the particles are round. The results are shown in Figure 3.

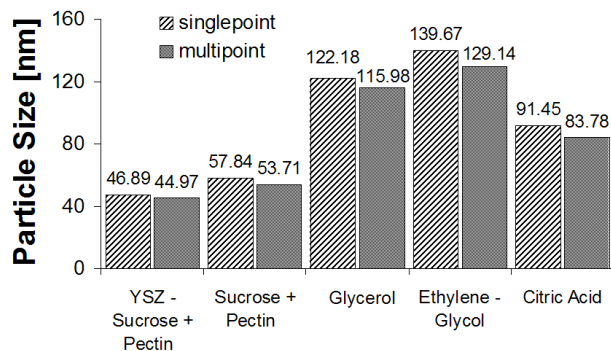
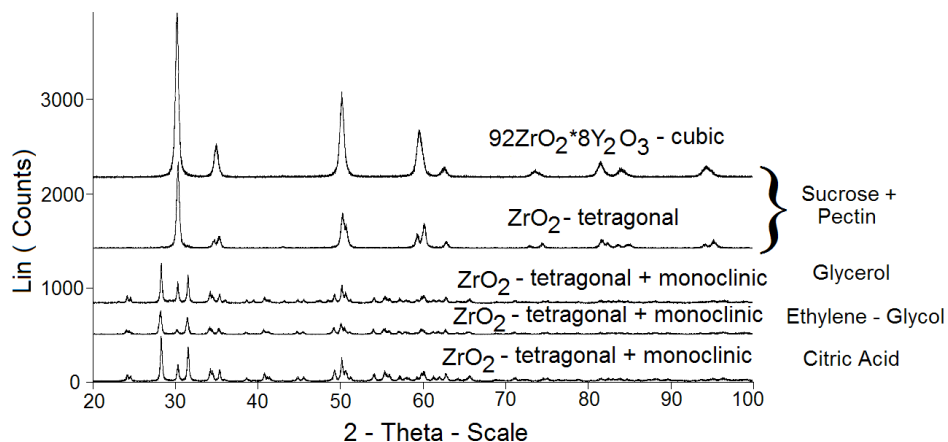


Fig. 3. The particle size of the samples according to BET analysis

3.3 X-Ray Diffraction

The X-ray diffraction spectra shown in Figure 4 obtained by Bruker D-8 Advance X-ray diffractometer in the $2-\theta$ range $20-100^\circ$. Spectra of the ZrO_2 samples using citric acid, ethylene glycol, and glycerol at temperature of $900^\circ C$ showed that the obtained nanoparticles consist of a mixture of ZrO_2 monoclinic and tetragonal phases. Patterns no. 50-1089 and 24-1165 correspond to zirconium oxide tetragonal and baddeleyite monoclinic according to the International Center for Diffraction Data (ICDD). In the case of ZrO_2 nanoparticles using sucrose/pectin mixture the XRD spectra showed the presence of the tetragonal phase corresponding to pattern no. 50-1089. The presence of other phase such as monoclinic zirconia was not observed in this sample. In the case of YSZ samples using sucrose/pectin organic precursor the XRD data indicated $92ZrO_2 \cdot 8Y_2O_3$ in only a single phase. The pattern 30-1468 corresponds to cubic yttrium zirconium oxide - $Y_{0.15}Zr_{0.85}O_{1.93} - 92ZrO_2 \cdot 8Y_2O_3$. The presence of other phases such as monoclinic or tetragonal zirconia or of free Y_2O_3 was not observed. Thus, can be assumed that a homogeneous solid solution of Y_2O_3 with ZrO_2 was formed.



030 - 1468 - Yttrium Zirconium Oxide - 8YSZ - Cubic
 050 - 1089 - Zirconium Oxide - ZrO_2 - Tetragonal
 024 - 1165 - Baddeleyite - ZrO_2 - Monoclinic

Fig. 4. The X-Ray spectra of the samples at $900^\circ C$

The Scherrer formula ($D = (k \lambda)/(B \cos\theta)$) was applied to the first four peaks of the obtained XRD spectra in order to determine the crystallite size of the powders. k is a constant, here taken as 0.94, λ is the wavelength of CuKalpha1, taken as 0.15406 nm, B is the width of the peak (FWHM) in radians, and $2-\theta$ is the angle of the mode of the peak. The Full Width at Half Maximum (FWHM) and the $2-\theta$ values determined from the XRD spectrum together with the calculated crystallite size of the samples. The mean crystallite size of the samples are shown in Figure 5.

The crystallite sizes obtained from the different peaks were reasonably consistent, the standard deviation of the mean values reported in the figure were, from left to right, 2.37, 12.24, 4.11, 9.62, 3.13 nm, respectively.

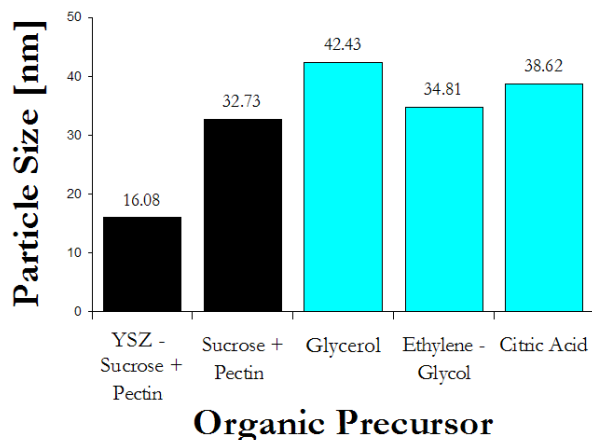


Fig. 5. The mean crystallite size of the samples

3.4 Transmission Electron Microscopy

A JEOL-JEM-1011 electron transmission microscope was used to examine all the samples (see Figure 6). Formvar powder (Agar Scientific LTD, Essex) dissolved in chloroform was used as an organic layer to cover the copper grids of the microscope, whereafter the grids were subjected to a carbon deposition process under vacuum followed by a glow discharge. The obtained powders were dispersed in distilled water under stirring and one drop taken from the solution was deposited on the grid. The TEM images show relatively uniform and spherical shapes with a narrow size distribution for the samples using citric acid and sucrose/pectin organic precursors. In the case of ethylene glycol and glycerol large agglomerates in which the individual particles are hardly distinguishable can be observed. The medium particle size calculated based on the TEM images are around 20–25nm for the sucrose/pectin samples, and 50–60nm for the citric acid ethylene glycol and glycerol samples.

4 Conclusion

In this paper we compared the nanoparticles produced using a sucrose/pectin gelification process with those produced using conventional organic precursors. The sucrose/pectin process is a fast, cheap, and easy to scale up chemical way for obtaining ZrO_2 and 8YSZ nanoparticles. The obtained nanoparticles using the new sol-gel precursors are smaller than the ones obtained with conventional organic precursors.

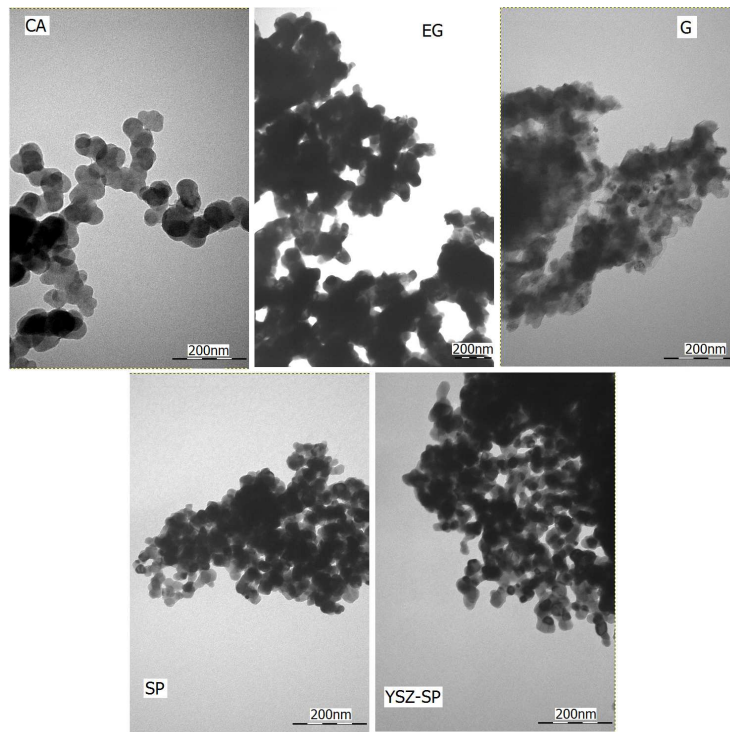


Fig. 6. The TEM images of the samples at 900°C

The appearance of a tetragonal phase in the four ZrO_2 powders is interesting, and may reflect a metastable phase in line with some of the studies quoted in the Introduction [12; 13]. The fact that *only* the tetragonal phase is present in the sucrose/pectin-derived powder may either be due to the particles being smaller, encouraging further the tetragonal metastable phase [13], or stabilization of the tetragonal phase by some impurity present in the organic precursor.

References

- [1] V. M. Rusu, C.-H. Ng, M. Wilke, B. Tiersch, P. Fratzl, M. G. Peter, Size-controlled hydroxyapatite nanoparticles as self-organized organic-inorganic composite materials, *Biomaterials* 27 (2005) 5414–5426.
- [2] D. Adityawarman, A. Voigt, P. Veit, K. Sundmacher, Precipitation of $BaSO_4$ nanoparticles in a non-ionic microemulsion: Identification of suitable control parameters, *Chem Eng Sci* 60 (2005) 3373–3381.
- [3] F. Guangneng, H. Lixia, H. Xueguang, Synthesis of single-crystal $BaTiO_3$ nanoparticles via a one-step sol-precipitation route, *Journal of Crystal Growth* 279 (2005) 489–493.
- [4] R. Arulmurugan, B. Jeyadevan, G. Vaidyanathan, S. Sendhilnathan, Effect of zinc substitution on Co-Zn and Mn-Zn ferrite nanoparticles prepared by co-precipitation, *Journal of Magnetism and Magnetic Materials* 288 (2005) 470–477.

- [5] W.-C. Hsu, S. C. Chen, P. C. Kuo, C. T. Lie, W. S. Tsai, Preparation of NiCuZn ferrite nanoparticles from chemical co-precipitation method and the magnetic properties after sintering, *Journal of Magnetism and Magnetic Materials B* 111 (2004) 142–149.
- [6] A. A. Ismail, Synthesis and characterization of $Y_2O_3/Fe_2O_3/TiO_2$ nanoparticles by sol-gel method, *Applied Catalysis B: Environmental* 58 (2005) 115–121.
- [7] G. Liu, X. Zhang, Y. Xu, X. Niu, L. Zheng, X. Ding, The preparation of Zn^{2+} -doped TiO_2 nanoparticles by sol-gel and solid phase reaction methods respectively and their photocatalytic activities, *Chemosphere* 59 (2005) 1367–1371.
- [8] Z. Xiu, M. Lü, S. Liu, G. Zhou, B. Su, H. Zhang, Barium hydroxyapatite nanoparticles synthesized by citric acid sol-gel combustion method, *Materials Research Bulletin* 40 (2005) 1617–1622.
- [9] D. R. Acosta, O. Novaro, T. Lopez, R. Gomez, Crystalline phases of sol-gel ZrO_2 in the ZrO_2-SiO_2 system—differential thermal-analysis and electron-microscopy studies, *Journal of Materials Research* 10 (1995) 1397–1402.
- [10] F. Gonella, G. Mattei, P. Mazzoldi, G. Battaglin, A. Quaranta, G. De, M. Montecchi, Structural and optical properties of silver-doped zirconia and mixed zirconia-silica matrices obtained by sol-gel processing, *Chemistry of Materials* 11 (1999) 814–821.
- [11] D. H. Aguilar, L. C. Torres-Gonzalez, L. M. Torres-Martinez, T. Lopez, P. Quintana, A study of the crystallization of ZrO_2 in the sol-gel system: ZrO_2-SiO_2 , *Journal of Solid State Chemistry* 158 (2001) 349–357.
- [12] C. L. Ong, J. Wang, L. M. Gan, S. C. Ng, Crystallization in nanosized sol-derived zirconia precursors, *Journal of Materials Science Letters* 15 (1996) 1680–1683.
- [13] V. R. Oleshko, J. M. Howe, S. Shukla, S. Seal, High-resolution and analytical tem investigation of metastable-tetragonal phase stabilization in undoped nanocrystalline zirconia, *Journal of Nanoscience and Nanotechnology* 4 (2004) 867–875.
- [14] K. Mehta, R. Xu, A. V. Virkar, Two-layer fuel cell electrolyte structure by sol-gel processing, *Journal of sol-gel science and technology* 11 (1997) 203–207.